Entrainment of Coupled Oscillators on Regular Networks by Pacemakers

Filippo Radicchi* and Hildegard Meyer-Ortmanns†
School of Engineering and Science,
International University Bremen,
P.O.Box 750561, D-28725 Bremen, Germany

We study Kuramoto oscillators, driven by one pacemaker, on d-dimensional regular topologies with nearest neighbor interactions. We derive the analytical expressions for the common frequency in the case of phase-locked motion and for the critical frequency of the pacemaker, placed at an arbitrary position in the lattice, so that above the critical frequency no phase-locked motion is possible. We show that the mere change in topology from an open chain to a ring induces synchronization for a certain range of pacemaker frequencies and couplings, while keeping the other parameters fixed. Moreover we demonstrate numerically that the critical frequency of the pacemaker decreases as a power of the linear size of the lattice with an exponent equal to the dimension of the system. This leads in particular to the conclusion that for infinite-dimensional topologies the critical frequency for having entrainment decreases exponentially with the size of the system, or, more generally, with the depth of the network, that is the average distance of the oscillators from the pacemaker.

PACS numbers: 05.45.Xt, 05.70.Fh

I. INTRODUCTION

Synchronization is an ubiquitous phenomenon, found in a variety of natural systems like fireflies [1], chirping crickets [2], or neural systems, but it is also utilized for artificial systems of information science in order to enable a well-coordinated behavior in time [3]. As an important special case, the coordinated behavior refers to similar or even identical units like oscillators that are individually characterized by their phases and amplitudes. A further reduction in the description was proposed by Kuramoto for an ensemble of oscillators [4], after Winfree had started with a first model of coupled oscillators [5]. Within a perturbative approach Kuramoto showed that for any system of weakly coupled and nearly identical limit-cycle oscillators, the long-term dynamics is described by differential equations just for the phases (not for the amplitudes) with mutual interactions, depending on the phase differences in a bounded form. It is this model, later named after him, that nowadays plays the role of a paradigm for weakly and continuously interacting oscillators. In a large number of succeeding publications the original Kuramoto model was generalized in various directions, for a recent review see [6]. In particular the natural frequencies were specialized in a way that one oscillator plays the role of a pacemaker with frequency higher than the natural frequencies of all other oscillators [7][8]. Pacemakers play an important role for the formation of patterns in Belousov-Zhabotinsky system [9]. Special families of wave solutions of the phases arise as a consequence of dynamically created pacemakers [4] [10]. Moreover pacemakers are important for the functioning of the heart [5] and for the collective behavior of *Dictyostelium discoideum* [11], as well as for large-scale ecosystems [12]. In [13] it is shown that a single periodic pendulum oscillator can entrain or at least drastically influence the dynamics of all chaotic pendula on two-dimensional lattices. Furthermore in [8] the role of pacemakers on complex topologies was analyzed in order to understand the functioning of the neural network at the basis of the circadian rhythm in mammals.

In this paper we consider a system of Kuramoto oscillators, coupled with their nearest neighbors on various regular lattice topologies, and driven by a pacemaker, placed at an arbitrary site of the lattice (section II). In particular, we analytically derive the common frequency of phase-locked motion in case of generic networks (in particular for d-dimensional regular lattices with open or periodic boundaries) in section III. Locked phases will be also called phase entrainment throughout this paper. We also analytically derive the upper bound on the absolute value of the ratio of the pacemaker's frequency to the coupling strength in case of one-dimensional regular lattices (section IV). In section V we consider higher-dimensional lattices and extend the results obtained for $d = 1$ to any dimension $d \geq 2$ of the lattice. We find that the range of pacemaker frequencies for which one obtains synchronization, the so-called entrainment window, decreases with an inverse power of the linear size N of the lattice with an exponent given by the dimension d of the lattice. This leads to the conclusion that the entrainment window of an infinite-dimensional network decreases exponentially with its linear size N if the pacemaker is asymmetrically coupled to the other oscillators. This conclusion is supported by our analysis of coupled oscillators on a Cayley-tree, a topology that amounts to an infinite-dimensional regular lattice. These results confirm the results recently obtained by Kori and Mikhailov [8] for random network topologies. For random topologies the entrainment window decays exponentially with the so-called depth of the network, that is the average

*f.radicchi@iu-bremen.de
†h.ortmanns@iu-bremen.de

distance of all other oscillators from the pacemaker. For our regular topologies, the linear size of the networks for hypercubic lattices and the radius of the Cayley tree are proportional to the network depth.

II. THE MODEL

The system is defined on a regular network. To each node i, $i = 0, \ldots, N$, we assign a limit-cycle oscillator, characterized by its phase φ_i that follows the dynamics

$$\dot{\varphi}_i = \omega + \delta_{i,s}\Delta\omega + (1+\delta_{i,s}\epsilon)\frac{K}{k_i}\sum_j A_{j,i}\sin(\varphi_j - \varphi_i) \quad . \tag{1}$$

A is the adjacency matrix of the system ($A_{i,j} = A_{j,i} = 1$ if the nodes i and j are connected and $A_{i,j} = 0$ otherwise), it reflects the underlying topology of the network. Here only nearest neighbors are coupled. Moreover, $k_i = \sum_j A_{j,i}$ is the degree of the i-th node, it gives the total number of connections of this node in the network. $\delta_{i,j}$ denotes the Kronecker delta ($\delta_{i,j} = 1$ if $i = j$ and $\delta_{i,j} = 0$ if $i \neq j$). The oscillator at position s represents the pacemaker. Its natural frequency differs by $\Delta\omega$ with respect to the natural frequency ω of all other oscillators. Without loss of generality we set $\omega = 0$, because system (1) is invariant under the transformation $\varphi_i \to \varphi_i + \omega t$, $\forall i$. Moreover the interaction of the pacemaker with the other oscillators can be linearly tuned by the parameter $-1 \leq \epsilon \leq 0$. For $\epsilon = 0$ the pacemaker is on the same footing as the other oscillators. For $\epsilon = -1$ its interaction is asymmetric in the sense that the pacemaker influences the other oscillators, but not *vice versa* (the pacemaker acts like an external force). In natural systems both extreme cases as well as intermediate couplings can be realized. The constant $K > 0$ parameterizes the coupling strength. The phases of the i-th and j-th oscillators interact via the sine function of their difference, as originally proposed by Kuramoto.

III. PHASE-LOCKED MOTION

We consider the conditions for having phase-locked motion , in which the phase differences between any pair of oscillators remain constant over time, after an initial short transient time. First we calculate the frequency Ω, in common to all oscillators in the phase-locked state. Imposing the phase-locked condition $\dot{\varphi}_i \equiv \Omega \quad , \forall\ i = 0, \ldots, N$ to system (1) and using the fact that the sine is an odd function (see the Appendix A for details), we obtain

$$\Omega \;=\; \Delta\omega\,\frac{k_s}{(1+\epsilon)\sum_{i\neq s} k_i + k_s} \quad . \tag{2}$$

As long as Ω depends on the degree k_s we see that the common frequency Ω increases with the degree of the pacemaker. On the other hand, when the network has a homogeneous degree of connections, $k_i \equiv k \quad , \forall\ i = 0, \ldots, N$, Eq.(2) takes the form

$$\Omega = \frac{\Delta\omega}{(1+\epsilon)\,N + 1} \quad . \tag{3}$$

It should be noticed that in this case the common frequency does not depend on the common degree k of the network.
In terms of the original parameterization of the model (1), the common frequency after synchronization is $\Omega+\omega$. For the derivation of Eq.s (2) and (3) we made only use of the odd parity of the coupling function. The former results are still valid for any other odd coupling function $f(\varphi_j - \varphi_j)$ which is 2π-periodic and bounded.

IV. ONE-DIMENSIONAL LATTICE

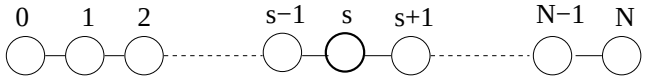

Figure 1: One-dimensional lattice with $N+1$ sites labelled by their coordinates.

A. Linear chain

Let us consider first the case of $N+1$ Kuramoto oscillators coupled along a chain (Figure 1) with free boundary conditions at the positions 0 and N ($k_i = 1$ if $i = 0$ or $i = N$, $k_i = 2$ otherwise), the pacemaker located at position s, $0 \leq s \leq N$. In this case it is convenient to introduce the phase lag between nearest neighbors $\theta_i = \varphi_i - \varphi_{i-1}$. Consider first the pacemaker placed at position $0 < s < N$. We start with the nearest oscillators to the right of the pacemaker, placed at position $i = s+1$

$$\begin{array}{l} \Omega = K/2\ [\ \sin(-\theta_{s+1}) + \sin(\theta_{s+2})\ ] \\ \Rightarrow \sin(\theta_{s+2}) = 2\Omega/K + \sin(\theta_{s+1}) \end{array} \quad .$$

Moving again to the right, the equation of the $(s+2)$-th oscillator reads

$$\begin{array}{l} \Omega = K/2\ [\ \sin(-\theta_{s+2}) + \sin(\theta_{s+3})\ ] \\ \Rightarrow \sin(\theta_{s+3}) = 2\Omega/K + \sin(\theta_{s+2}) \\ \Rightarrow \sin(\theta_{s+3}) = 4\Omega/K + \sin(\theta_{s+1}) \end{array} \quad .$$

Iteratively, we can write for each $1 \leq j \leq N - s$

$$\sin(\theta_{s+j}) = 2\,(j-1)\,\frac{\Omega}{K} + \sin(\theta_{s+1}) \quad . \tag{4}$$

In particular when $j = N - s$ we have

$$\sin(\theta_N) = 2\,(N-s-1)\,\frac{\Omega}{K} + \sin(\theta_{s+1}) \quad ,$$

but also at the boundary

$$\Omega = K \sin(-\theta_N) \quad .$$

From the last two equations we can simply determine the value of $\sin(\theta_{s+1})$ as function of s, N and Ω. Substituting this value into Eq.(4), we obtain

$$\sin(\theta_{s+j}) \;=\; 2(j-1)\frac{\Omega}{K} \;+\; (2s-2N+1)\,\frac{\Omega}{K}\,. \qquad (5)$$

When $\Omega > 0$ ($\Omega < 0$), Eq.(5) is always negative (positive) and has its minimum (maximum) value for $j = 1$. This means that when the pacemaker succeeds in "convincing" its nearest neighbors to the right to adapt his frequency, all the others to the right do the same. Now, the absolute value of the critical threshold can be calculated by only using the fact that the sine function is bounded ($|\sin(\theta)| \leq 1$) and using the expression for Ω as a function of ϵ and N, as it is derived in the Appendix A in Eq.(A2)

$${}^{R}\left|\frac{\Delta\omega}{K}\right|_C = \frac{(1+\epsilon)\,N-\epsilon}{2N-2s-1} \quad . \qquad (6)$$

Eq.(6) yields the bound for oscillators to the right (R) of s to approach a phase-locked state. Following the same procedure, but moving to the left of the pacemaker, we find

$${}^{L}\left|\frac{\Delta\omega}{K}\right|_C = \frac{(1+\epsilon)\,N-\epsilon}{2s-1} \qquad (7)$$

as bound for oscillators to the left (L) of the pacemaker to synchronize in a phase-locked motion. Since we are interested in a state with all oscillators of the chain being phase-entrained, we need the stronger condition given by

$$\left|\frac{\Delta\omega}{K}\right|_C = \min\left[\,{}^{R}\left|\frac{\Delta\omega}{K}\right|_C\,,\,{}^{L}\left|\frac{\Delta\omega}{K}\right|_C\,\right] \quad . \qquad (8)$$

For the pacemaker placed at the boundaries $s = 0$ or $s = N$, using Eqs.(2) and (A2), we obtain

$$\left|\frac{\Delta\omega}{K}\right|_C = \frac{(1+\epsilon)\,(2N-1)+1}{2N-1} \quad . \qquad (9)$$

B. Ring topology

If we close the chain of $N+1$ oscillators to a ring, $k_i \equiv 2$, $\forall i$, the derivation of the upper bound on the pacemaker's frequency $|\Delta\omega/K|_C$ proceeds in analogy to that of Eq.(9). Using Eq.(3), the final result is then given as

$$\left|\frac{\Delta\omega}{K}\right|_C \;=\; \frac{1}{N} + (1+\epsilon) \quad . \qquad (10)$$

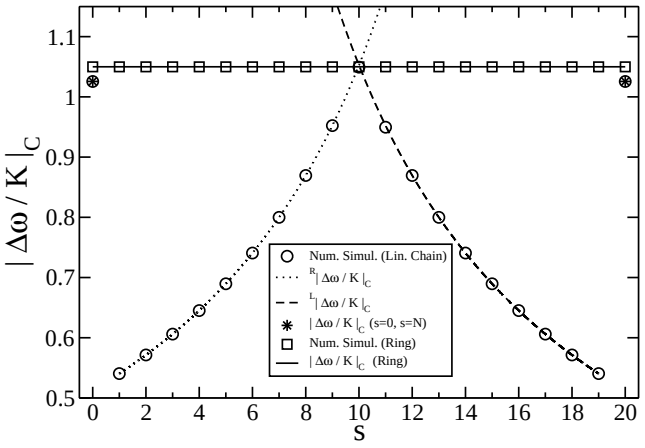

Figure 2: Critical threshold $|\Delta\omega/K|_C$ as function of the position s of the pacemaker on a one-dimensional lattice. For further details see the text.

In all former cases, for $N \to \infty$, the critical threshold $|\Delta\omega/K|_C$ goes to $(1+\epsilon)$ [or values proportional to $(1+\epsilon)$]. Differently, the common frequency Ω goes to ω for $0 \geq \epsilon > -1$ and $N \to \infty$, while Ω goes to $\omega + \Delta\omega$ for $\epsilon = -1$ and $N \to \infty$. Therefore the symmetric coupling of the pacemaker to the rest of the system favors the synchronizability of the system, while it can no longer synchronize for a completely asymmetric coupling of the pacemaker ($\epsilon = -1$). This is plausible as it must be easier for N oscillators to convince one pacemaker to follow them (case $\epsilon > -1$) than the opposite case, in which the pacemaker must convince N oscillators to follow it (case $\epsilon = -1$). For increasing system size, the latter case becomes impossible, while the former is still possible.

C. Topological switch to synchronization

The numerical results of this paper are obtained by integrating the set of Eq.s(1) with the Runge-Kutta method of fourth order ($dt = 0.1$). The numerical value of the critical threshold $|\Delta\omega/K|_C$ is evaluated with an accuracy of $5 \cdot 10^{-5}$. As one knows from [4], in case of regular topologies, stable solutions with different winding numbers are possible. To avoid different winding numbers, we always choose homogeneous initial conditions (also the distribution of *phases* would be different in particular in the synchronized state).
We summarize the results obtained so far in Figure 2. The analytical results for $|\Delta\omega/K|_C$ are represented by lines for the open chain [dotted line from Eq.(6) and dashed line from Eq.(7)], for the ring [full line from Eq.(10)] and by crosses [Eq.(9)] in case of an open chain with the pacemaker at the boundaries, while the circles (open chain) and squares (ring) represent numerical data that reproduce the analytical predictions within the nu-

merical accuracy. All results are obtained for $N = 20$ and $\epsilon = 0$, they are plotted as a function of the pacemaker's position s that only matters in case of the open chain. The horizontal line obviously refers to the ring, the two branches (left and right), obtained for the chain, cross this line when the pacemaker is placed at $s = 10$ in the middle of the chain. When the pacemaker is located at the boundaries $s = 0$ and $s = 20$, we obtain two isolated data points close to the horizontal line.

Let us imagine that for given N and ϵ the absolute value of the pacemaker's frequency $|\Delta\omega|$ and the coupling K are specified out of a range, such that the ratio is too large to allow for phase-locked motion on a chain, but small enough to allow the phase-entrainment on a ring. It is then the mere closure of the open chain to a ring that leads from non-synchronized to synchronized oscillators with phase-locked motion. Therefore, for a whole range of ratios $|\Delta\omega/K|$, no finetuning is needed to switch to a synchronized state, but just a simple change in topology, the closure of a chain to a ring. Because this closure may be much easier feasible in real systems than a fine tuning of parameters to achieve synchronization, we believe that this mechanism is realized in natural systems and should be utilized in artificial ones. In our numerical integration we simulated such a switch and plot the phase portrait in Figure 3. The phases φ_i as function of time are always projected to the interval $[0, 2\pi)$: we use a thick black line for the phase of the pacemaker and thin dark-grey lines for the other oscillators. In this concrete numerical simulation with $T \cdot dt = 4000$ integration steps altogether, we analyzed a one-dimensional lattice of Kuramoto oscillators with $N = 6$, $s = 2$, $\Delta\omega/K = 1$ and $\epsilon = 0$. In the time interval from 0 to "ON" $(T/3)$ we see a phase evolution with different slopes and varying with time. Moreover, the pacemaker and the left part of the system (oscillators $i = 0, 1$) have larger frequencies than the right part of the system (oscillators $i = 3, 4, 5, 6$). At the instant "ON" we close the chain, passing to a ring topology, the system almost instantaneously reaches a phase-locked motion (all phases moving with the same and constant frequency). At time "OFF" $(2T/3)$ we open the ring, again, the system then behaves similarly to the first phase, i.e. for $t \in [0, ON)$. Furthermore it should be

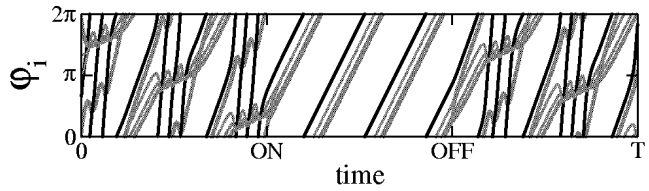

Figure 3: Phase portrait of a system of Kuramoto oscillators on a one-dimensional lattice. This figure shows how it is possible to switch "ON" and "OFF" synchronization via a simple topological change of the system, passing from a linear chain to a ring and vice versa. A more detailed description is given in the text.

noticed from Figure 2 that it is also favorable to put the pacemaker at the boundaries of an open chain to facilitate synchronization. For $d = 1$ the pacemaker then has to entrain only one rather than two nearest neighbors so that the range of allowed frequencies $|\Delta\omega|$ increases.

V. HIGHER DIMENSIONS

All of our results obtained so far extend qualitatively to higher dimensions d, when system (1) is placed on a hypercubic lattice with $(N_j + 1)$ oscillators in each direction j, so that we have an ensemble of $\Pi_{j=1}^{d}(N_j + 1)$ Kuramoto oscillators, where the i-th oscillator's position is labelled by a d-dimensional vector $\vec{i}$, with $0 \leq i_j \leq N_j$, $\forall\ j = 1, \ldots, d$. If the condition for having a phase-locked motion is satisfied, the system of oscillators reaches a common frequency still given by Eq.(2). Such condition now is satisfied for $|\Delta\omega/K| \leq |\Delta\omega/K|_C$, the critical ratio for the pacemaker's frequency at position $\vec{s} = (s_1, \ldots, s_d)$[see Figure 4]. In the simplest case when

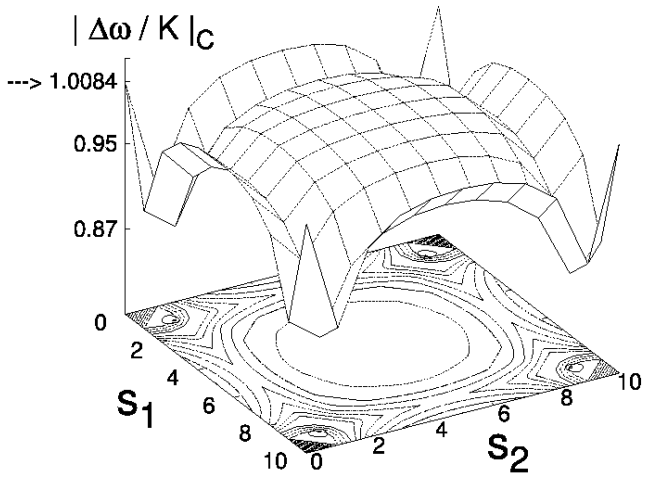

Figure 4: Same as Figure 2, but in $d = 2$ dimensions. The linear size of the system is $N = 10$. The arrow indicates the value of the critical threshold for periodic boundary conditions.

the lattice has $(N + 1)$ sites in each direction, we can qualitatively extend all the previous results, obtained so far for $d = 1$, to any dimension $d \geq 2$. For example, the "closure" of the open boundaries of the lattice to a torus in d dimensions favors synchronization of the system. We checked this numerically for $d = 2$ and $N = 10$ [Figure 4]. Except for the central node at $\vec{s} = (5, 5)$, the critical threshold in case of open boundary conditions lies always below that for periodic boundary conditions. Moreover, it is natural to assume that the former results, obtained for one-dimensional lattices, in the case of periodic boundary conditions extend to d-dimensional lattices by replacing N in Eq.(10) by $(N + 1)^d - 1$

$$\left|\frac{\Delta\omega}{K}\right|_C = \frac{1}{(N+1)^d - 1} + (1 + \epsilon) \quad . \tag{11}$$

For $\epsilon = -1$ and fixed K, the entrainment window $\Delta\omega_c$

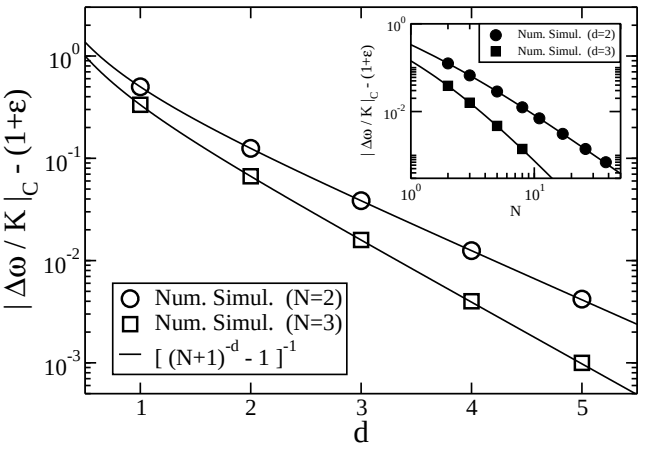

Figure 5: Entrainment window for higher dimensional lattices. We plot the critical threshold $|\Delta\omega/K|_C - (1+\epsilon)$ that is independent on ϵ as it is seen from Eq.(11). The main plot shows the dependence of the entrainment window on the dimension d, while the inset shows its dependence on the linear size N of the lattice. Numerical results are plotted as symbols. They fit perfectly with our predictions according to Eq.(11).

decreases exponentially with the dimension d of the lattice and as a power of the linear size of the lattice with exponent d. This conjecture is supported by the numerical results as documented in Figure 5. For this reason we expect that for infinite-dimensional systems ($d \to \infty$) the entrainment window decreases exponentially with the linear size of the system if the pacemaker is asymmetrically coupled with $\epsilon = -1$.

In order to verify this conjecture, we study a system of limit-cycle oscillators placed on a Cayley tree [Figure 6]. Cayley trees have z branches to nearest neighbors at each node, apart from nodes in the outermost shell, where the number of nearest neighbors is $z-1$. Cayley trees are infinite-dimensional objects in the sense that the surface of the system (i.e. the number of nodes in the outermost shell at distance R from the the center) is proportional to the volume of the system (i.e. the total number of nodes in the tree). The set of evolution equations is still given by Eq.(1), with the adjacency matrix A specialized to the underlying Cayley tree topology. For simplicity, we consider only the case of the pacemaker placed at the center of the tree ($s = 0$).

When the number of branches per nodes z is two, the Cayley tree becomes a linear chain, with $N = 2R$ and the pacemaker placed at position $s = N/2 = R$. Obviously for $z = 2$ we find the same results as given in the previous section (see the Appendix B).

The infinite dimensionality of the tree shows up for $z > 2$. We obtain

$$\Omega = \Delta\omega \, \frac{z-2}{z-2+(1+\epsilon)\left[2(z-1)^R - z\right]} \qquad (12)$$

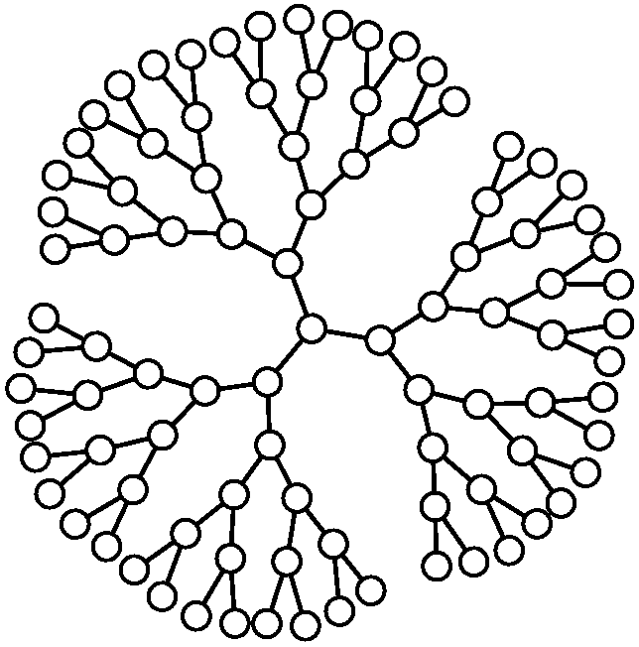

Figure 6: Cayley tree with $z = 3$ branches and radius $R = 5$.

as common frequency for the phase-locked motion and

$$\left|\frac{\Delta\omega}{K}\right|_C = \frac{z-2}{2\,(z-1)^R - z} + (1+\epsilon) \qquad (13)$$

as critical ratio for obtaining the phase-locked motion. Both Eq.s (12) and (13) are valid for $R \geq 2$. In particular Eq.(13) tell us that for $\epsilon = -1$ the entrainment window *decreases exponentially* with the radius R of the Cayley tree (see Figure 7). For large $z \geq 2$ it is easily seen that the radius R gets proportional to the depth D of the network (in the limit $z \gg 2$ one finds $D \simeq R$). These results nicely confirm those recently obtained by Kori and Mikhailov [8], who found that in infinite-dimensional systems such as random networks and small-world networks with a high number of rewired edges, the entrainment window decreases exponentially with the depth of the network. In order to connect their results to ours, we note that not only the radius R of the Cayley tree, but also the linear size N of the hypercubic lattices are proportional to the depth of these regular networks.

VI. SUMMARY AND CONCLUSIONS

Entrainment of Kuramoto oscillators, coupled on regular lattices via a pacemaker is possible for large system sizes ($N \to \infty$) only in the case of symmetric ($\epsilon = 0$) couplings of the pacemaker. As the pacemaker coupling becomes asymmetric ($-1 \leq \epsilon < 0$), synchronization becomes more and more difficult, and impossible for large system sizes and $\epsilon = -1$. However, we are not only interested in the "thermodynamic" limit. For finite N and $-1 \leq \epsilon \leq 0$, we find that for a whole range of ratios

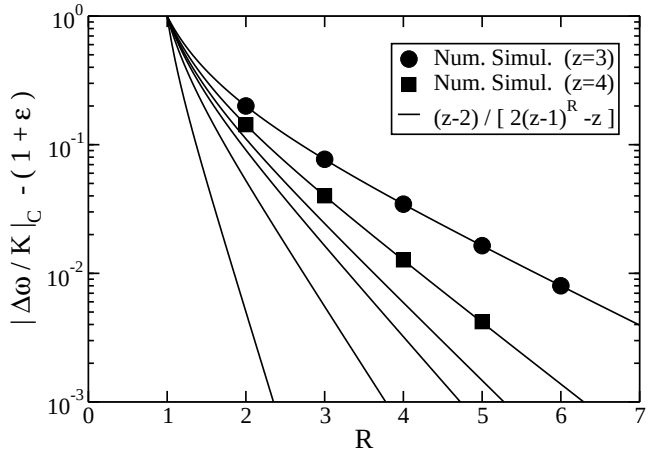

Figure 7: Entrainment window for Cayley trees as a function of the radius R. Numerical results (full dots and squares) refer to $z = 3$ and 4. The full lines correspond to plots of $|\Delta\omega/K|_C - (1+\epsilon)$, as defined in Eq.(13), for different coordination numbers z, from up to down $z = 3, 4, 5, 6, 10$ and 100, respectively.

$|\Delta\omega/K|$ it is possible to induce synchronization by a mere closure of a chain to a ring. The sensitive dependence of synchronization on the topology in a certain range of parameters may be exploited in artificial networks and is -very likely- already utilized in natural systems, in which a switch to a synchronized state should be easily feasible (although we are currently not aware of a concrete example from biological systems). If the pacemaker is coupled symmetrically to the other oscillators ($\epsilon = 0$), the entrainment window stays finite in the large-N limit, but the common frequency approaches zero for $N \to \infty$. In the other extreme case, if the pacemaker is coupled asymmetrically to the rest of the system ($\epsilon = -1$), our main result is that the entrainment window decreases as a power of the depth of the network with the dimension d in the exponent. Extrapolating this behavior to arbitrary dimension d, we see that one of the reasons of the exponentially fast "closure" of the entrainment window in complex network topologies [8] is their effective infinite dimensionality.

Appendix A: COMMON FREQUENCY

Imposing the phase-locked condition, setting $\omega = 0$ and dividing by $K/k_i, \forall\ i = 0, \ldots, N$, system (1) takes the form

$$\frac{k_i}{K}\Omega \;=\; \delta_{i,s}\frac{k_i}{K}\Delta\omega \;+\; (1+\delta_{i,s}\epsilon)\,\Omega_i \quad , \qquad \text{(A1)}$$

where

$$\Omega_i \;:=\; \sum_{j\neq i}\sin\left(\varphi_j - \varphi_i\right) \quad .$$

From the odd parity of the sine function it follows that

$$\sum_i \Omega_i = 0 \quad \text{and} \quad \sum_{i\neq g}\Omega_i = -\Omega_g \quad .$$

Summing (A1) over all i except $i = s$ we obtain

$$\begin{array}{l} \sum_{i\neq s}\Omega\frac{k_i}{K} = \sum_{i\neq s}\delta_{i,s}\frac{k_i\Delta\omega}{K} + \sum_{i\neq s}(1+\delta_{i,s}\epsilon)\,\Omega_i \\ \Rightarrow \frac{\Omega}{K}\sum_{i\neq s}k_i = -\Omega_s \end{array} ,$$

while summing (A1) over all i except $i = j$, where $j \neq s$, we obtain

$$\begin{array}{l} \sum_{i\neq j}\Omega\frac{k_i}{K} = \sum_{i\neq j}\delta_{i,s}\frac{k_i\Delta\omega}{K} + \sum_{i\neq j}(1+\delta_{i,s}\epsilon)\Omega_i \\ \Rightarrow\ \frac{\Omega}{K}\sum_{i\neq j}k_i = \frac{k_s\Delta\omega}{K} - \Omega_j + \epsilon\Omega_s \\ \Rightarrow\ \frac{\Omega}{K}\sum_{j\neq s}\sum_{i\neq j}k_i = \sum_{j\neq s}\frac{k_s\Delta\omega}{K} - \sum_{j\neq s}\Omega_j + \sum_{j\neq s}\epsilon\Omega_s \\ \Rightarrow\ \frac{\Omega}{K}\sum_{j\neq s}\sum_{i\neq j}k_i = \frac{Nk_s\Delta\omega}{K} + (1+\epsilon N)\Omega_s \end{array} .$$

It should be noticed that

$$\sum_{j\neq s}\sum_{i\neq j}k_i = Nk_s + (N-1)\sum_{i\neq s}k_i \quad ,$$

so that we can write

$$\Omega\left[(1+\epsilon)\sum_{i\neq s}k_i + k_s\right] = k_s\Delta\omega \quad ,$$

from which Eq.(2) is implied.
In the case of a one-dimensional lattice with open boundary conditions, we have $k_0 = 1 = k_N$ and $k_j = 2$, $\forall j \neq 0, N$, so that

$$\sum_{i\neq s}k_i \;= \begin{cases} 2N-1 & \text{, if } s = 0 \text{ or } s = N \\ 2\,(N-1) & \text{, otherwise} \end{cases} .$$

The common frequency of Eq.(2) can be written as

$$\Omega \;=\; \Delta\omega \begin{cases} \frac{1}{(1+\epsilon)(2N-1)+1} & \text{, if } s = 0 \text{ or } s = N \\ \frac{1}{(1+\epsilon)(N-1)+1} & \text{, otherwise} \end{cases} . \quad \text{(A2)}$$

Appendix B: COMMON FREQUENCY AND CRITICAL THRESHOLD FOR CAYLEY TREES

Consider a node in the outermost shell, i.e. at distance R from the pacemaker, reached along the path $\vec{s}_R = (s_1, s_2, s_3, \ldots, s_{R-1}, s_R)$ from the central node. Here $s_1 = 1, \ldots, z$, while $s_i = 1, \ldots, z-1$, $\forall i = 2, \ldots, R$ [see Figure 6] label the choice of branch along the path. For this node we can write Eq.s (1) as

$$\begin{array}{l} \dot{\varphi}_{\vec{s}_R} = \Omega = \\ = K\sin\left(\varphi_{\vec{s}_{R-1}} - \varphi_{\vec{s}_R}\right) \\ \Rightarrow\ \sin\left(\varphi_{\vec{s}_{R-1}} - \varphi_{\vec{s}_R}\right) = \frac{\Omega}{K} \end{array} ,$$

from which we can see that all oscillators at distance R, independently on the path along which they are reached from the center, satisfy the same equation.
Proceeding in an analogous way as before, we find for the shell $R-1$

$$\dot{\varphi}_{\vec{s}_{R-1}} = \Omega =$$
$$= \frac{K}{z}\Big[\sum_{s_R=1}^{z-1} \sin\left(\varphi_{\vec{s}_R} - \varphi_{\vec{s}_{R-1}}\right) +$$
$$+ \sin\left(\varphi_{\vec{s}_{R-2}} - \varphi_{\vec{s}_{R-1}}\right)\Big] =$$
$$= \frac{K}{z}\Big[-(z-1)\frac{\Omega}{K} + \sin\left(\varphi_{\vec{s}_{R-2}} - \varphi_{\vec{s}_{R-1}}\right)\Big]$$
$$\Rightarrow \sin\left(\varphi_{\vec{s}_{R-2}} - \varphi_{\vec{s}_{R-1}}\right) = \frac{\Omega}{K}[z + (z-1)] \,.$$

Furthermore, for the shell $R-2$ we obtain

$$\dot{\varphi}_{\vec{s}_{R-2}} = \Omega =$$
$$\frac{K}{z}\Big[\sum_{s_{R-1}=1}^{z-1} \sin\left(\varphi_{\vec{s}_{R-1}} - \varphi_{\vec{s}_{R-2}}\right) +$$
$$+ \sin\left(\varphi_{\vec{s}_{R-3}} - \varphi_{\vec{s}_{R-2}}\right)\Big] =$$
$$= \frac{K}{z}\Big[-(z-1)\frac{\Omega}{K}[z + (z-1)] + \sin\left(\varphi_{\vec{s}_{R-3}} - \varphi_{\vec{s}_{R-2}}\right)\Big]$$
$$\Rightarrow \sin\left(\varphi_{\vec{s}_{R-3}} - \varphi_{\vec{s}_{R-2}}\right) = \frac{\Omega}{K}\left[z + z(z-1) + (z-1)^2\right]$$

until we arrive for $R-(t+1)$ at

$$\sin\left(\varphi_{\vec{s}_{R-(t+1)}} - \varphi_{\vec{s}_{R-t}}\right) = \frac{\Omega}{K}\left[z\sum_{q=0}^{t-1}(z-1)^q + (z-1)^t\right] \,.$$

For $t = R-1$, we have

$$\sin\left(\varphi_{\vec{s}_0} - \varphi_{\vec{s}_1}\right) = \frac{\Omega}{K}\left[z\sum_{q=0}^{R-2}(z-1)^q + (z-1)^{R-1}\right] \,,$$

but also, at the center of the Cayley tree,

$$\Omega = \dot{\varphi}_{\vec{s}_0} =$$
$$= \Delta\omega + (1+\epsilon)\,\frac{K}{z}\sum_{s_1=1}^{z}\sin\left(\varphi_{\vec{s}_1} - \varphi_{\vec{s}_0}\right) = \,,$$
$$= \Delta\omega - (1+\epsilon)\,\Omega\left[z\sum_{q=0}^{R-2}(z-1)^q + (z-1)^{R-1}\right]$$

from which

$$\Omega = \Delta\omega\left[1 + (1+\epsilon)\left(z\sum_{q=0}^{R-2}(z-1)^q + (z-1)^{R-1}\right)\right]^{-1} \,. \tag{B1}$$

For $z = 2$ the Cayley tree reduces to a linear chain with $N+1$ oscillators ($N = 2R$), open boundary conditions and the pacemaker placed at position $s = N/2$. The common frequency given in Eq.(B1) becomes the same as in Eq.(A2).
For $z > 2$ we can rewrite the truncated geometric series as

$$\sum_{q=0}^{R-2}(z-1)^q = \frac{(z-1)^{R-1} - 1}{z-2} \tag{B2}$$

and obtain after some algebra Eq.(12).
As we have seen, all oscillators at the same distance r from the pacemaker satisfy the same equation. We can write

$$\sin\left(\varphi_r - \varphi_{r-1}\right) = -\frac{\Omega}{K}\left[z\sum_{q=0}^{R-r-1}(z-1)^q + (z-1)^{R-r}\right] \,, \tag{B3}$$

suppressing the path that was followed to reach the node. From Eq.(12) it is easily seen that when $\Omega > 0$ [$\Omega < 0$], Eq.(B3) is always negative [positive], monotone and increasing [decreasing] and takes its minimum [maximum] value for $r = 1$. Imposing the bound of the sine function ($|\sin(\varphi)| \leq 1$) to Eq.(B3), with $r = 1$, and inserting Eq.(B1) we obtain

$$\left|\frac{\Delta\omega}{K}\right|_C = \frac{1}{z\sum_{q=0}^{R-2}(z-1)^q + (z-1)^{R-1}} + (1+\epsilon) \,.$$

For $z = 2$ again we obtain Eq.s(6) and (7) with $s = N/2$. For $z > 2$ we can again use the truncated geometric series of Eq.(B2) and obtain Eq.(13).

[1] J. Buck , Nature **211** , 562 (1966).
[2] T.J. Walker , Science **166** , 891 (1969).
[3] I. Kanter , W. Kinzel , and E. Kanter , Europhys. Lett. **57** , 141 (2002).
[4] Y. Kuramoto , *"Chemical Oscillators, Waves, and Turbolence"* , (Springer New York 1984).
[5] A.T. Winfree , *"The geometry of biological time"* , (Springer-Verlag New York 1980).
[6] J.A. Acebrón , L.L. Bonilla , C.J. Pérez-Vicente , F. Ritort , and R. Spigler , Rev. Mod. Phys. **77** , 137 (2005).
[7] H. Yamada , Prog. Theor. Phys. **108** , 13 (2002).
[8] H. Kori , and A.S. Mikhailov , Phys. Rev. Lett. **93** , 254101 (2004).
[9] A.N. Zaikin , and A.M. Zhabotinsky , Nature **225** , 535 (1970).
[10] B. Blasius , and R.Tönjes , Phys. Rev. Lett. **95** , 084101

(2005) ; Y. Kuramoto , and T. Yamada , Prog. Theor. Phys. **56** , 724 (1976).
[11] K.J. Lee , E.C. Cox , and R.E. Goldstein , Phys. Rev. Lett. **76** , 1174 (1996).
[12] B. Blasius , A. Huppert, and L. Stone , Nature (London) **399** , 354 (1999).
[13] M. Weiss , T. Kottos , and T. Geisel , Phys. Rev. E **63** , 056211 (2001).